

# Magnetostatic Spin-Wave Modes in Ferromagnetic Tube

Alexander Kozhanov<sup>1</sup>, Daniel Ouellette<sup>2</sup>, Mark Rodwell<sup>3</sup>, Dok Won Lee<sup>4</sup>, Shan X. Wang<sup>5</sup>, and S. J. Allen<sup>2</sup>

<sup>1</sup>California Nano Systems Institute, University of California at Santa Barbara, Santa Barbara, CA 93106 USA

<sup>2</sup>Physics Department, University of California at Santa Barbara, Santa Barbara, CA 93106-9530 USA

<sup>3</sup>Department of Electrical Engineering, University of California at Santa Barbara, Santa Barbara, CA 93106 USA

<sup>4</sup>Stanford University, Stanford, CA 94305 USA

<sup>5</sup>Geballe Laboratory for Advanced Materials, Stanford University, Stanford, CA 94305 USA

**Magnetostatic spin-wave modes were excited and detected in micron size ferromagnetic  $\text{Co}_{90}\text{Ta}_5\text{Zr}_5$  rectangular tubes that wrapped around the shorted ends of coplanar waveguides. The observed modes can be assigned to surface spin waves of an infinite ferromagnetic film but with periodic boundary conditions and quantized wave vector imposed by the finite circumference of the tube.**

**Index Terms**—Ferromagnetic tubes, spin waves, tunable filters.

## I. INTRODUCTION

**S**MALL-SCALE magnetostatic spin-wave devices are potentially important for on-chip filters for communication systems [1]–[3], inductors [4], [5], and spin-wave logic devices [6], [7]. Recent theoretical [8]–[10] and experimental [11] work has focused on magnetization dynamics in ferromagnetic nanotubes.

Yttrium iron garnet is a well-known material used for delay lines, tunable filters, and other magnetostatic signal processing devices and has been intensively explored and used for such applications [12]. However, ferromagnetic metal films such as CoFe, CoFeB, or CoTaZr, with larger saturation magnetization, permit higher frequency operation [13]. Further, these materials are rather easily processed and integrated with existing semiconductor technology. High conductivity of these materials results in eddy current damping of the magnetization oscillation, but can be eliminated by using very thin films or by laminating or dicing.

In this work, we experimentally explore spin waves in hollow  $\text{Co}_{90}\text{Zr}_5\text{Ta}_5$  rectangular tubes using a structure shown schematically in Fig. 1.

## II. EXPERIMENTAL SETUP

Ferromagnetic  $\text{Co}_{90}\text{Zr}_5\text{Ta}_5$  films (200 nm thick, saturation magnetization  $M_S = 1.2$  T) were sputtered onto Si/SiO<sub>2</sub> wafers and lithographically patterned into two  $6\ \mu\text{m} \times 10\ \mu\text{m}$  rectangles which were covered with 100-nm insulating SiO<sub>2</sub> layer. 100-nm-thick aluminum coupling loops formed by a shorted coplanar waveguides were placed over  $\text{Co}_{90}\text{Zr}_5\text{Ta}_5$  rectangles as seen in Fig. 1. After covering with 100-nm-thick SiO<sub>2</sub> and etching appropriate holes, a top layer of 200-nm  $\text{Co}_{90}\text{Zr}_5\text{Ta}_5$  was sputtered and patterned by liftoff to complete the tube. As a result, we obtained two shorted coplanar waveguides tied with a  $\text{Co}_{90}\text{Zr}_5\text{Ta}_5$  film wrapped around the

Manuscript received March 06, 2009. Current version published September 18, 2009. Corresponding author: A. Kozhanov (e-mail: kozhanov@cnsi.ucsb.edu).

Color versions of one or more of the figures in this paper are available online at <http://ieeexplore.ieee.org>.

Digital Object Identifier 10.1109/TMAG.2009.2023919

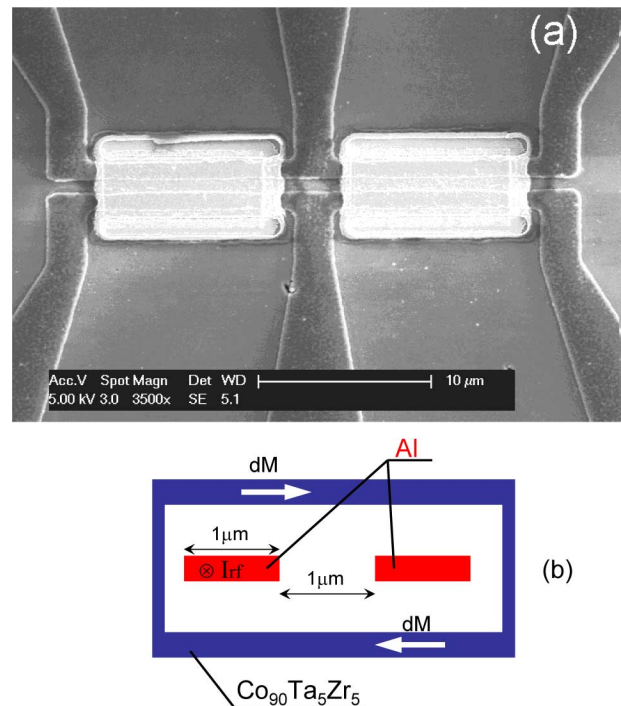


Fig. 1. (a) SEM micrograph of fabricated structure. (b) Fabricated structure cross section scheme.

short-circuit ends. The use of two tubes instead of one was aimed at symmetrical current distribution in the shorted ends of coplanar waveguide and enhanced coupling between exciting and detecting waveguides. Since the  $\text{Co}_{90}\text{Zr}_5\text{Ta}_5$  film forms a closed magnetic circuit around exciting and detecting coupling loops, transmission through such structure should be strongly dependent on the spin-wave modes of the magnetic tube.

$S$ -parameters were measured at room temperature using Agilent 8720ES vector network analyzer in frequency range 0.05–20 GHz. Only  $S_{21}$ , the ratio of high-frequency voltage at terminals 2 to the input high-frequency voltage at terminals 1, is analyzed in the following discussion. The test devices were positioned on the narrow gap of small electromagnet that provided bias up to 1000 Oe along the axis of the tube. By comparing the  $S$ -parameters at disparate bias magnetic fields, the magnetic field-independent instrument response

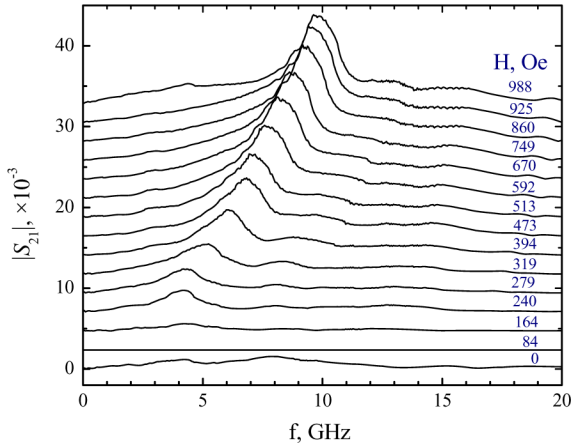


Fig. 2. Frequency dependence of  $|S_{21}|$  measured on fabricated structure at different applied magnetic fields.

can be effectively removed to expose the  $S$ -parameters of the magnetostatic spin-waves-coupled coplanar waveguides.

We were able to observe several transmission peaks in  $|S_{21}|$  (Fig. 2) that depended on the applied magnetic field. In the absence of an external magnetic field,  $|S_{21}|$  has a number of peaks with a magnitude of  $\sim 10^{-3}$ . With increasing external magnetic field directed along the axis of the tube, the magnitude of these peaks decreased and magnetic coupling almost disappeared at  $H \sim 100$  Oe. Further increase of the external magnetic field results in appearance of a series of  $|S_{21}|$  peaks which shift towards higher frequencies with increase of  $H$ . The amplitude of the major peak reaches  $|S_{21}| \sim 10^{-2}$  at  $H \sim 1000$  Oe. The amplitude of the higher frequency peaks is about ten times smaller. The low amplitude of transmitted signal is caused by the impedance mismatch of the coplanar waveguide and its shortened ends so most of the exciting signal is being reflected.

Micromagnetic simulations show that in zero external magnetic field magnetization prefers to be circularly oriented around the tube perimeter. This geometry is not favorable for efficient magnetization excitation since the exciting magnetic field is parallel to the magnetic moments in the tube. That results in a very weak magnetic coupling between exciting and detecting coupling loops at  $H = 0$ . Increasing the magnetic field applied to the tube results in reorientation of magnetic moments; and at  $H \sim 100$  Oe the peaks in  $|S_{21}|(f)$  disappear.

Further increase of the magnetic field aligns all magnetic moments along the tube resulting in the appearance of spin-wave modes related to the axially magnetized ferromagnetic tube starting from magnetic field  $H \sim 200$  Oe.

The peaks observed at  $H > 200$  Oe shift towards higher frequencies with increasing  $H$ . Dependence of the peak frequencies versus  $H$  is shown in Fig. 3. The thin film ferromagnetic resonance magnetic field dependence nicely lays over the lowest frequency peak observed in our experiment.

Magnetic field dependence of the higher frequency peaks could be fit with surface waves of an infinite plane, but with

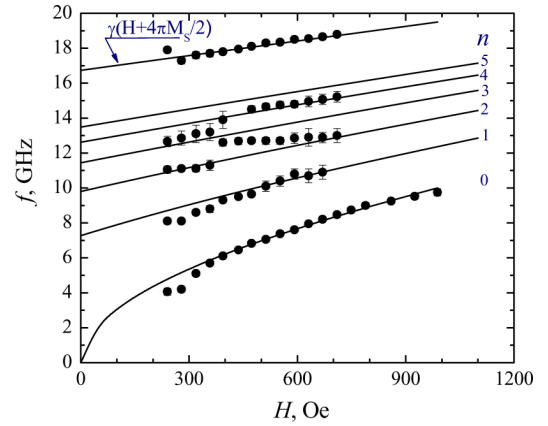


Fig. 3. Frequency dependence of  $|S_{21}|$  peaks on the applied magnetic.

wave vector quantized by  $\lambda_n = L/n$ , where  $L$  is the perimeter of the tube

$$f(H) = \gamma \sqrt{H(H + M_s) + \frac{M_s^2}{4}(1 - e^{-2k_n d})} \quad (1)$$

where  $k_n = 2\pi/\lambda_n$  is a wave vector,  $H$  is applied magnetic field,  $M_s$  is saturation magnetization,  $d$  is the film thickness, and  $\gamma$  is the gyromagnetic ratio [14].

Although the tube is far from circular, we find quantitative agreement by using the actual perimeter  $L \approx 12 \mu\text{m}$ . Apparently, the closed topology is sufficient to give a good agreement with the experiment although the shape is hardly a perfect cylindrical tube.

The highest frequency peak that we observe in the experimental data fits with the top of the surface wave band, which behaves as  $f \sim \gamma(H + 4\pi M_s/2)$ .

### III. CONCLUSION

In summary, we have coupled high-frequency coplanar waveguides by magnetostatic spin waves in ferromagnetic  $\text{Co}_{90}\text{Zr}_5\text{Ta}_5$  metal tubes. At  $H < 100$  Oe, transmission of fabricated structure is very weak due to circular orientation of magnetization in the tube. Increase of the external magnetic field reorients its magnetization along the tube axis. At fields higher than 200 Oe, we are able to identify a ferromagnetic resonance (FMR) mode and surface spin-wave modes with spin-wave vector quantized so that whole number of wavelengths would fit in the tube perimeter.

This may be an approach to high-frequency tunable filters controlled by external magnetic fields or with a direct current (dc) flowing through the exciting and detecting loops.

### ACKNOWLEDGMENT

The authors would like to thank A. Cleland for the use of the vector network analyzer and hosting aspects of this work in his laboratory. This work was supported by Nano Electronics Research Corporation (NERC) via the Nanoelectronics Research

Initiative (NRI), Intel Corporation, and the University of California Discovery at the Western Institute of Nanoelectronics (WIN) Center.

#### REFERENCES

- [1] J. D. Adam, "Analog signal processing with microwave magnetics," *Proc. IEEE*, vol. 76, no. 2, pp. 159–170, Feb. 1988.
- [2] W. S. Ishak, "Magnetostatic wave technology: Review," *Proc. IEEE*, vol. 76, no. 2, pp. 171–187, Feb. 1988.
- [3] C. S. Tsai, J. Su, and C. C. Lee, "Wideband electronically tunable microwave bandstop filters using iron film-gallium arsenide waveguide structures," *IEEE Trans. Magn.*, vol. 35, no. 5, pp. 3178–3180, Sep. 1999.
- [4] D. S. Gardner, G. Schrom, P. Hazucha, F. Paillet, T. Karnik, and S. Borkar, "Integrated on-chip inductors with magnetic films," *IEEE Trans. Magn.*, vol. 43, no. 6, pp. 2615–2617, Jun. 2007.
- [5] A. M. Crawford, D. Gardner, and S. X. Wang, "High-frequency microinductors with amorphous magnetic ground planes," *IEEE Trans. Magn.*, vol. 38, no. 5, pp. 3168–3170, Sep. 2002.
- [6] D. A. Allwood, G. Xiong, C. C. Faulkner, D. Atkinson, D. Petit, and R. P. Cowburn, "Magnetic domain-wall logic: A review," *Science*, vol. 309, no. 5741, pp. 1688–1692, 2005.
- [7] M. P. Kostylev, A. A. Serga, T. Schneider, B. Leven, and B. Hillebrands, "Spin wave logical gates," *Appl. Phys. Lett.*, vol. 87, pp. 153501-1–153501-3, 2005.
- [8] M. A. Popov and I. V. Zavislyak, "Modelling of magnetostatic surface oscillations in elliptic nanotubes," *Ukrainian J. Physics*, vol. 53, no. 7, pp. 702–707, 2008.
- [9] T. M. Nguyen and M. G. Cottam, "Spin-wave excitations in ferromagnetic nanotubes," *Surface Sci.*, vol. 600, pp. 4151–4154, 2006.
- [10] H. Leblond and V. Veerakumar, "Magnetostatic spin solitons in ferromagnetic nanotubes," *Phys. Rev. B, Condens. Matter*, vol. 70, pp. 134413-1–134413-7, 2004.
- [11] S. Mendach, J. Podbelski, J. Topp, W. Hansen, and D. Heitmann, "Spin-wave confinement in rolled-up ferromagnetic tubes," *Appl. Phys. Lett.*, vol. 93, pp. 262501-1–262501-3, 2008.
- [12] J. D. Adam, L. E. Davis, G. F. Dionne, E. F. Schloemann, and S. N. Stitzer, "Ferrite devices and materials: A review," *IEEE Trans. Microw. Theory. Tech.*, vol. 50, no. 3, pp. 721–737, Mar. 2002.
- [13] B. Kuanr, I. R. Harward, D. L. Marvin, T. Fal, R. E. Camley, D. L. Mills, and Z. Celinski, "High-frequency signal processing using ferromagnetic metals," *IEEE Trans. Magn.*, vol. 41, no. 10, pp. 3538–3543, Oct. 2005.
- [14] R. W. Damon and J. R. Eshbach, "Magnetostatic modes of a ferromagnetic slab," *J. Chem. Phys. Solids*, vol. 19, no. 3/4, pp. 308–320, 1961.